Eur. Phys. J. D **36**, 67–78 (2005)
DOI: 10.1140/epjd/e2005-00182-9

THE EUROPEAN PHYSICAL JOURNAL D

Role of the chemical ordering on the magnetic properties of Fe–Ni cluster alloys

R.A. Guirado-López[1,2,a], M.C. Desjonquères[1,b], and D. Spanjaard[3,c]

[1] CEA/DSM/DRECAM/SPCSI, CE de Saclay, 91191 Gif-sur-Yvette, France
[2] Instituto de Física "Manuel Sandoval Vallarta", Universidad Autónoma de San Luis Potosí, Alvaro Obregón 64, 78000 San Luis Potosí, México
[3] Laboratoire de Physique des Solides, Bâtiment 510, Université Paris-Sud, Centre d'Orsay, 91405 Orsay, France

Received 3 March 2005
Published online 12 July 2005 –

Abstract. The spin and orbital moments of fcc Fe−Ni cluster alloys are determined within the framework of a *d*-band Hamiltonian including the spin-orbit coupling non perturbatively. Different sizes (up to 321 atoms), compositions, and chemical configurations (random alloys as well as core-shell arrays of iron and nickel atoms) are considered in order to reveal the crucial role played by local order and stoichiometry on the magnetic moments of the clusters. Interestingly, we have found considerably reduced average magnetizations for Fe−Ni clusters with Fe cores compared to that of the bulk alloy with the same composition. Indeed, in these configurations not only antiparallel arrangements between the local moments of some Fe atoms within the iron core are found, but also the total magnetization of the surface Ni atoms is significantly quenched. On the opposite, the disordered and Ni-core cluster alloys are characterized by high magnetizations resulting from saturated-like contributions from both Ni and Fe atoms, in agreement with recent ab-initio calculations. In general, the local orbital magnetic moments are strongly enhanced with respect to their bulk values. Finally, the variation of the orbital-to-spin moment ratio with the chemical order is discussed.

PACS. 73.22.-f Electronic structure of nanoscale materials: clusters, nanoparticles, nanotubes, and nanocrystals – 61.46.+w Nanoscale materials: clusters, nanoparticles, nanotubes, and nanocrystals – 75.75.+a Magnetic properties of nanostructures

1 Introduction

An important contribution to the remarkable progress in nanoparticle magnetism is well-known to come from the development of advanced manufacturing techniques such as gas evaporation experiments [1], colloidal chemistry strategies [2], and electrodeposition techniques [3] which have allowed the fabrication of a large variety of pure and alloyed particles with different sizes and morphologies having contrasting properties. Besides the importance of studying still open problems on basic research, nanoparticle systems have been found to be also attractive due to their applications on chemical catalysis, optical devices, and magnetic recording. Intensive experimental studies have clearly shown that the characterization and control of their microstructure and chemical composition are of fundamental importance for a complete understanding of the observed macroscopic behavior and that small variations of these quantities can lead to the existence of novel phenomena.

It is generally believed, on the basis of experimental data and theoretical calculations, that the magnetic moment (per atom) of nanoparticles is enhanced compared to the bulk value due to the reduced dimensionality and strong surface contributions. This is observed, not only for pure metal clusters, for example of ferromagnetic elements (Ni [4], Co [5]) or of elements which are not magnetic in the bulk and magnetic in clusters (Rh for instance [6]), but also for alloys. As a representative example of the last case we would like to mention the recent magnetic measurements performed by Zitoun et al. [7] on bimetallic Co−Rh clusters synthesized by means of an organometallic precursor technique where it has been found that remarkably large magnetic fields of up to 30 T are not sufficient to fully saturate the magnetization of the nanoparticles. In fact, average magnetic moments of $\sim$2.3 μ_B/Co atom have been obtained in these clusters, that are considerably larger than the ones found in the bulk Co−Rh alloys [8], and even larger than the values obtained in the case of pure Co_N particles [9].

Recently, Li et al. [10] have synthesized ultra-fine Fe−Ni particles (with a mean diameter of 30–35 nm) of several chemical compositions by using the hydrogen

[a] e-mail: ricardo@drecam.saclay.cea.fr
[b] e-mail: mcdjs@drecam.saclay.cea.fr
[c] e-mail: spanjaard@lps.u-psud.fr

plasma reaction method and determined their structure and magnetization. Using the X-ray diffraction technique, they have shown that the structure of these nanoparticles remains fcc up to at least 60% of Fe content above which the bcc structure starts to appear. Surprisingly, they have found that the magnetic moment per atom in these clusters is much lower than that of the corresponding bulk samples in the whole range of compositions. This reduction of the magnetization is also observed for pure Ni and Fe nanoparticles. As suggested by Li et al., this low magnetization might be due to a non alignment of the magnetic moments of surface atoms in the applied field, or the existence or not of single domains. In addition, due to the preparation method, adsorbed gases are expected to be present on the surface, a fact that is well-known to lead, at least in most of the extended transition metal surfaces, to a sizable quenching of the local magnetization [e.g., H adsorption on Ni(001) thin films [11]]. However Li et al. pointed out that another source of reduction of magnetization should be present since the saturation magnetization does not increase significantly in the Fe−Ni cluster alloys with increasing Fe content as in the bulk samples. They also stated that this cannot be explained only by the existence of magnetically dead (or considerably quenched) surface layers since no obvious change in the mean particle size with the Fe content is observed.

This experimental study has motivated two theoretical works. We would like to mention first the work of Guevara et al. [12] who have investigated the magnetism of an fcc $Fe_{47}Ni_{178}$ cluster built from alternate shells of Fe and Ni atoms by using a tight-binding model Hamiltonian. They found, for their most stable solution, a ferromagnetic configuration with an average magnetic moment of 1.25 μ_B/atom, which is slightly larger than the bulk alloy value and cannot explain the experimental findings in Fe−Ni nanoparticles for that composition ($\sim$0.5 μ_B/atom). However they mentioned the existence of anti-ferromagnetic (AF) solutions close in energy. Later on, Rao et al. [13] have analyzed, by using a first-principle molecular-orbital approach, the magnetic and structural properties of very small Fe−Ni clusters with equi-atomic composition (having up to 8 atoms). They have obtained that the magnetic moment per atom in these alloys is almost insensitive to the specific geometry of the clusters and found average moments as large as 2.3 μ_B/atom, i.e., considerably enhanced with respect to the bulk alloy value for that composition. Furthermore, by considering cluster structures made of small fractions of the bcc lattice, the authors of reference [13] have analyzed the energetics and magnetic behavior of iron-rich clusters ($Fe_{n-1}Ni$ with $n = 9$, 15, 27 and Fe_7Ni_2). The average magnetic moment in all cases was found to be unaffected by the precise location of the Ni atom(s) within the structures and equal to 2.67 and 3.07 μ_B/atom for Fe_8Ni and $Fe_{14}Ni$ clusters respectively, which are values again enhanced with respect to both Fe−Ni bulk and nanoparticle measurements.

Thus, at least up to now, there is no explanation for the measurement of Li et al. However we believe that there are some important aspects not included in the previous theoretical modelling that make difficult the comparison with experimental findings. First, the size of the observed particles is much larger than the size that can be reached in any type of electronic structure calculations. Second, the effect of the possible existence of adsorbed gases on the external shell of the clusters needs to be considered. However, as clearly shown in the experimental work of Knickelbein and co-workers [14] and Cox et al. [15], that have analyzed the effect of hydrogen and oxygen adsorption, respectively, on the magnetic moments of Fe clusters, the correlation between the magnetic properties and the degree of surface contamination can be very subtle. Actually, unlike the case of thin films where adsorption of these molecules quenches the magnetic moment, in cluster systems these authors have found that the magnetic moments of hydrogenated or oxydized clusters could be higher than those of free clusters, being thus probably a source of either reduction or enhancement of the average magnetization. Third, the configuration of the synthesized Fe−Ni particles could be the result of a competition between thermodynamic and kinetic factors (due to the rapid condensation of the evaporated gases in the method of hydrogen plasma reaction). This fact might lead to the formation of unusual structural and chemical phases (completely different from the ones observed in the equilibrium Fe−Ni phase diagram) that could strongly affect the magnetic behavior, and it is actually the contribution of this separate effect that we would like to underline in the present contribution. Actually, the existing calculations have been limited to a given chemical order and the influence of a change of chemical order, for instance, the possible existence of a phase segregation, leading to nanoparticles of the core-shell type, has not been analyzed and may be of fundamental importance in determining the magnetic behavior observed on a macroscopic scale. Finally, it should be remarked that the previous semi-empirical and ab-initio calculations were restricted to analyze only the spin magnetization of the cluster and, as a consequence, the contribution of the orbital moments to the total magnetization in low dimensional systems and its complex behavior as a function of the local atomic environment have been neglected [16–18].

In the present work we have performed a systematic theoretical investigation of the magnetic properties of Fe−Ni cluster alloys by using a *d*-band tight-binding Hamiltonian treated in the unrestricted Hartree-Fock approximation, as proposed in reference [20], where the effects of the spin-orbit interaction (which allows us to calculate the orbital contributions to the total magnetization) are included non perturbatively. Concerning the cluster structures we assume [guided by X-ray diffraction (XRD) spectra reported in Ref. [10]] unrelaxed fcc fragments and, consequently, we limit ourselves to Fe contents smaller than 75%. For the reasons that we have discussed above, we have decided to analyze, for each one of the considered compositions, (1) Fe−Ni alloyed particles (in which starting from pure Ni, a gradual random substitution of the Ni atoms by Fe is performed) as well as (2) segregated clusters with a core-shell structure, namely, Fe at the core and Ni in the outer shells and vice-versa. In these

last cases, we will consider both ideal core-shell Fe−Ni nanoparticles (characterized by a perfect separation of species) as well as structures having different degrees of intermixing at the Fe−Ni interface. Special attention is paid on the local distribution of the magnetic moments in the particles (both spin and orbital contributions) and with this analysis we have been able to observe well defined chemical configurations that can considerably reduce the total magnetization of the system. In particular this reduction of the magnetic moment per atom begins to appear in Fe core structures when the size of the core is not too small. This trend is revealed by complete calculations, i.e., including spin-orbit coupling, on 19 and 43 atom cluster alloys. It is confirmed by the study of larger clusters (up to 321 atoms) which have been carried out neglecting the spin-orbit coupling to make the calculations tractable since we have found that the main effect comes from the spin polarization. Even if within the considered theoretical framework we are not able to determine the most stable chemical configuration in our cluster alloys, we believe that the strong correlation between chemical order and magnetic behavior in Fe−Ni cluster alloys could play an important role in the magnetization data reported by Li et al. The rest of the paper is organized as follows. In Section 2 we briefly describe the theoretical model used for the calculations. In Section 3 we present the discussion of our results and finally, in Section 4 the summary and conclusions are given.

2 Theoretical model

Self-consistent semiempirical calculations have been performed for several Fe−Ni cluster alloys by using the realistic d-band tight-binding Hamiltonian, proposed in reference [20], which includes the intra-atomic Coulomb interactions in the unrestricted Hartree-Fock approximation and the effects of the spin-orbit coupling non perturbatively. The model has been described in detail elsewhere [21,22], thus we only summarize its main points.

Due to the inclusion of the spin-orbit (SO) interaction, the rotational invariance of the electronic Hamiltonian is no longer preserved and depends now on the orientation δ of the magnetization in the system. In the usual notation the Hamiltonian is given by

$$H^{\delta} = \sum_{i\lambda,\sigma} \Delta\epsilon^{\delta}_{i\sigma} n_{i\lambda\sigma} + \sum_{i\lambda,j\mu,i\neq j,\sigma} t_{i\lambda,j\mu} c^{+}_{i\lambda\sigma} c_{j\mu\sigma} + \sum_{i,\lambda\sigma,\mu\sigma'} \xi_i (\boldsymbol{L}_i \cdot \boldsymbol{S}_i)_{\lambda\sigma,\mu\sigma'} c^{+}_{i\lambda\sigma} c_{i\mu\sigma'}, \quad (1)$$

where $c^{+}_{i\lambda\sigma}(c_{i\lambda\sigma})$ refers to the creation (annihilation) operator of an electron with spin σ in the d orbital λ at atomic site i and $n_{i\lambda\sigma} = c^{+}_{i\lambda\sigma} c_{i\lambda\sigma}$ defines the electron number operator. The first term of equation (1), $\Delta\epsilon^{\delta}_{i\sigma}$ corresponds to the site- and spin-dependent energy shift of the d level $\epsilon_{i\sigma} = \epsilon^{0}_{d} + \Delta\epsilon^{\delta}_{i\sigma}$ (where ϵ^{0}_{d} stands for the d orbital energy in the paramagnetic bulk) and is determined by the global charge and the spin as follows

$$\Delta\epsilon^{\delta}_{i\sigma} = U(i)\Delta n^{\delta}(i) - \sigma J(i) S_{\delta}(i), \quad (2)$$

with $\Delta n^{\delta}(i) = n^{\delta}(i) - n_d(\text{bulk})$. The average intra-atomic direct Coulomb repulsion integral is denoted by U and the average exchange integral is denoted by J. The spin-quantization axis is taken to be parallel to the magnetization direction, which is assumed to be uniform within the cluster. In the second term of equation (1) $t_{i\lambda,j\mu}$ denotes the corresponding hopping integrals between sites i and j and orbitals λ and μ and finally, the third term corresponds to the spin-orbit interaction treated in the usual intra-atomic single-site approximation [23,24]. Here, ξ_i stands for the SO coupling constant at atom i (i.e., ξ_{Fe} and ξ_{Ni}) and $(\boldsymbol{L}_i \cdot \boldsymbol{S}_i)_{\lambda\sigma,\mu\sigma'}$ refer to the intra-atomic matrix elements of $\boldsymbol{L} \cdot \boldsymbol{S}$ which couple the up and down spin-manifolds and which depend on the relative orientation between the magnetization direction and the cluster lattice. The number of d-electrons at site i,

$$n^{\delta}(i) = \sum_{\lambda} \left(\langle n^{\delta}_{i\lambda\uparrow} \rangle + \langle n^{\delta}_{i\lambda\downarrow} \rangle \right), \quad (3)$$

and the local spin $\boldsymbol{S}(i) = [S_x(i), S_y(i), S_z(i)]$ at each cluster site i and for a given direction of magnetization δ,

$$S_{\delta}(i) = \frac{1}{2} \sum_{\lambda} \left(\langle n^{\delta}_{i\lambda\uparrow} \rangle - \langle n^{\delta}_{i\lambda\downarrow} \rangle \right), \quad (4)$$

are calculated self-consistently by integrating the local density of states (LDOS) $\rho^{\delta}_{i\lambda\sigma}(\varepsilon) = -(1/\pi)\text{Im}\{G^{\delta}_{i\lambda\sigma,i\lambda\sigma}(\varepsilon)\}$, where $G^{\delta}(\varepsilon) = [\varepsilon - H^{\delta}]^{-1}$ is the Green function operator, up to the Fermi level ε_F which is determined by the number of d electrons per atom in the clusters.

The local orbital moments $L_{\delta}(i)$ at each cluster site are calculated from

$$L_{\delta}(i) = \sum_{\sigma} \sum_{m=-2}^{m=2} \int_{-\infty}^{\varepsilon_F} m\, \rho^{\delta}_{im\sigma}(\varepsilon)\, d\varepsilon, \quad (5)$$

where the real d-orbitals have been transformed to the complex spherical harmonics basis and m refers to the magnetic quantum number. Here, the quantization axis of the orbital momentum is the same as the spin quantization axis.

The LDOS $\rho^{\delta}_{i\lambda\sigma}(\varepsilon)$ are determined by performing independent self consistent calculations for each orientation of the magnetization δ. In all cases, we will consider a magnetization direction, along the z-axis taken as a principal symmetry axis of the particle, as well as one in-plane direction within the xy-plane of the clusters, taken along a nearest neighbor bond. However, it is important to remark that the magnetization direction in the structures can be chosen without restrictions. The LDOS $\rho^{\delta}_{i\lambda\sigma}(\varepsilon)$ are computed by using Haydock-Heine-Kelly's recursion method [25]. The number of levels used in the continued fraction expansion of the Green's function is such that the results for $\rho^{\delta}_{i\lambda\sigma}(\varepsilon)$ correspond to the exact solution of the single-particle problem.

3 Results

The parameters used for the calculations on Fe−Ni cluster alloys are the following. The two-center d electron hopping integrals between atoms of the same element (i.e., Ni−Ni and Fe−Fe) are given by the canonical expression [26] in terms of the corresponding bulk d-band widths of the elements involved in the cluster alloys [27], namely: $W_b(\mathrm{Fe}) = 6.0$ eV and $W_b(\mathrm{Ni}) = 5.0$ eV. On the other hand, the heteronuclear hoppings integrals (Fe−Ni) are obtained as the geometric average of the corresponding homonuclear hopping integrals. This has been proved to be a very good approximation in calculations for embedded clusters [28], bulk alloys [29] and multilayers [30] of transition metals. The intra-atomic exchange integral J is chosen to yield the proper magnetic moment and exchange splittings in the bulk at $T = 0$ [$J(\mathrm{Fe}) = 0.67$ eV and $J(\mathrm{Ni}) = 0.5$ eV] with bulk d-band fillings of $n_d(\mathrm{Fe}) = 7.0$ and $n_d(\mathrm{Ni}) = 9.0$ as used in previous works [16,31]. Charge transfer effects are treated in the limit of large direct Coulomb repulsion U [i.e., $U(i) \to +\infty$ and $\Delta n^\delta(i) \to 0$ with $U(i)\Delta n^\delta(i)$ finite], which amounts to impose local charge neutrality at each site i. This approximation is well justified in this case due to the similar electronegativity of both elements, which is at the origin of the negligible charge transfer obtained in small Fe−Ni clusters [13], thin films [32], and bulk alloys [33]. Finally, the corresponding values of the SO coupling constants are taken from reference [24] [$\xi_{\mathrm{Fe}} = 0.05$ eV and $\xi_{\mathrm{Ni}} = 0.11$ eV].

Concerning the structure of our particles we use, following the XRD spectra of Fe−Ni nanoparticles of reference [10], bulk fcc fragments of 19, 43, 201, 249, and 321 atoms. We will consider low, medium, and high (however less than about 75%) concentrations of Fe atoms in the particles being 1) randomly distributed in the structure as well as 2) in segregated configurations (core-shell arrays) in which Fe can be at the core and Ni in the outer shells or vice versa (having both abrupt and alloyed interfaces), for the two previously mentioned orientations of the magnetization. In the following subsections we present and discuss our results.

3.1 Magnetic properties of fcc Ni_{19} and $FeNi_{18}$ clusters

We would like to show first our results for the magnetic properties of pure unrelaxed fcc Ni_{19} and single Fe-doped $FeNi_{18}$ clusters, in order to analyze the behavior of the local moment distribution across the particles and how this distribution is affected by the presence of a single Fe atom included as a substitutional impurity in the structure. No lattice relaxation effects were included and thus the cluster sites refer to the positions of an ideal small fragment of the fcc lattice with an interatomic distance of 2.5 Å, which corresponds to the bulk interatomic spacing of both Fe and Ni elements ($R_{\mathrm{Ni-Ni}} = R_{\mathrm{Fe-Fe}} = 2.50$ Å).

In Figure 1 we plot the decomposition of the local moment into spin $2S_\delta$ and total $M_\delta = 2S_\delta + L_\delta$ contributions at each site i of the fcc Ni_{19} cluster for two orientations

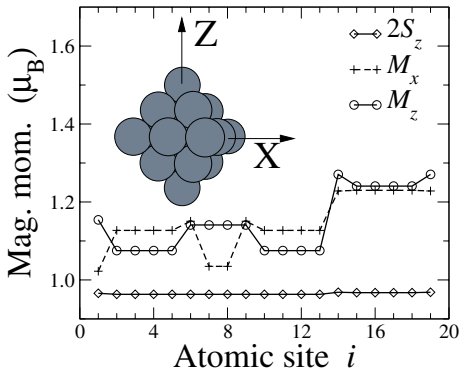

Fig. 1. Calculated local spin $2S_z(i)$ and total magnetic moments $M_\delta(i)$ for the fcc Ni_{19} cluster. In the inset we show the structure of the Ni_{19} cluster together with the two considered orientations of the magnetization. The central site is defined by $i = 1$, values from $i = 2-13$ specify atoms located at the first shell of neighbors, and sites with $i = 14-19$ define the outermost atomic shell.

of the magnetization as referred to in the inset. The central site is defined by $i = 1$, values from $i = 2-13$ specify atoms located at the first shell of neighbors around the central atom, and sites with $i = 14-19$ define the outermost atomic shell. First, we would like to comment that, in agreement with the results obtained in previous theoretical studies on surfaces [21], thin films [34], and small particles [20,35], the spin moments are found to depend very weakly on the direction of magnetization so we only refer here and in the following to the results for $2S_z$, which corresponds to the magnetization oriented along the z-axis of the particle. By looking at the behavior of $2S_z(i)$ at the different sites i we observe no sensitivity to the local atomic environment since the spin magnetic moments are nearly saturated ($\sim$0.96 μ_{B}), and are thus independent of the existing small intra-atomic redistributions of charge, the local coordination, and of the precise details of the electronic spectra (degeneracy, local d-band widths, etc.). A similar result has been reported at the fcc surfaces of Ni by both semiempirical [21] and ab-initio [36] calculations where the magnitude of $2S_z$ ($\sim$0.6 μ_{B}) has been found to be also almost independent of the open or closed-packed character of the surface layer and of the position of the Ni atoms in the structure (at the surface or at the inner planes). On the contrary, we note that the total local moment $M_\delta(i)$ depends significantly on the local atomic environment and on the direction of magnetization, due to the sizable orbital contributions, and is thus different for the different sites. As can be inferred from Figure 1, the values of $L_\delta(i)$ for the central and outer atoms can even differ by more than 500%, and also the variations at the inner sites are remarkable. In particular, it is important to note that geometrically equivalent sites in the cluster [i.e., atoms belonging to a given shell of neighbors ($i = 1$, 2–13, and 14–19)] can become inequivalent when the spin-orbit coupling is considered since the direction of the magnetization must be fixed and a preferential axis is introduced. Consequently, there is a lowering of the symmetry with respect to the geometrical one. For instance, when the

magnetization is along the z-axis, the sites $i = 6-9$ which belong to the $z = 0$ plane have the same value of L_z and which is different from that found for sites $i = 2-5$ and $i = 10-13$ which are themselves equivalent. Similarly, the second nearest neighbors of the central atom located in the $z = 0$ plane ($i = 15-18$) are equivalent but different from the two others ($i = 14$ and 19). However, as will be seen in the following sections, in the case of cluster alloys the symmetry can be completely destroyed or conserved to some degree, the latter case occurring for instance when the chemical configuration is such that there remains a rotational invariance with respect to the magnetization direction.

From Figure 1 we also note that, when compared with the measured values for the orbital moment in the bulk [37], $L^{exp}_{\rm bulk}({\rm Ni}) = 0.051\ \mu_{\rm B}$, a sizable enhancement is found at all the sites, being more pronounced at the atoms located at the outermost shell (as large as 600% for L_z). Actually, it is this complex structure of $L_\delta(i)$ vs. i that induces also a complex behavior for $M_\delta(i)$ $[M_\delta(i) = 2S_\delta(i) + L_\delta(i)]$ which is thus of fundamental importance for a realistic determination of the magnetization profile within the structure. The average orbital magnetic moment $\langle L_\delta \rangle \sim 0.18\ \mu_{\rm B}$/atom is thus an important contribution, is always parallel to the spin moment and thus adds to $2\langle S_\delta \rangle = 0.96\ \mu_{\rm B}$/atom representing about 16% of the total magnetization $\langle M_\delta \rangle$ of the Ni_{19} cluster. Similar enhancements for the orbital moments have been obtained in previous calculations for Ni_N clusters [16], where their importance for a quantitative comparison between theory and the experimental average magnetization data has been demonstrated.

The local spin moment distribution when a single Fe atom is introduced as a substitutional impurity in several different positions in the previous fcc Ni structure reveals also some interesting trends. The most important feature to remark is that the average spin moment in $FeNi_{18}$ clusters (1.07 $\mu_{\rm B}$/atom) is independent of the position of the Fe atom in the structure, being the result of saturated-like contributions from both Ni ($\sim$1.0 $\mu_{\rm B}$) and Fe ($\sim$3.0 $\mu_{\rm B}$) species. In our $FeNi_{18}$ clusters, the well defined value for the average spin magnetization can be understood in terms of the corresponding changes induced in the electronic spectra of the 19-atom structure with the inclusion and different locations of the Fe atom. Actually, by analyzing the average electronic density of states (not shown) of all configurations we have noticed that, even if significant removal of degeneracies as well as level inversions are obtained all along the electronic spectra in $FeNi_{18}$ clusters, the existing highly degenerated states for the up- and down-spin bands located around the Fermi level do not change their position with the location of the Fe atom within the structure. As a consequence, the total occupations for the up and down spin bands are practically always the same, giving thus an almost constant average spin moment. A similar result has been also obtained by Rao et al. [13] when analyzing the spin magnetization of a single Ni impurity in a bcc 15-atom iron structure, as well as of small equiatomic FeNi clusters, by means of first principles calculations, where the average spin magnetic moments were also unaffected by the precise location of the Ni and Fe atoms within the clusters.

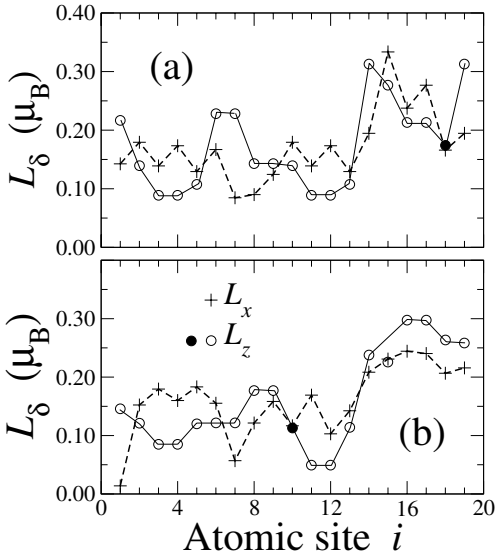

Fig. 2. Local orbital magnetic moments $L_\delta(i)$ as a function of the atom number i for two representative $FeNi_{18}$ clusters. The results shown in (a) and (b) correspond to atomic configurations in which an Fe atom is placed in the second and first shell of neighbors of the 19-atom structure, respectively. The values of $L_\delta(i)$ at the Fe sites are denoted by the filled circles.

Next, in Figures 2a and 2b, we plot representative results showing the behavior of the local orbital magnetic moments for two different positions (nearest and next-nearest neighbor of the central atom) of the Fe atom (denoted by a filled circle) within the 19-atom structure. From the figures we note that, contrary to the spin case, the orbital moments in both $FeNi_{18}$ clusters are very sensitive to the local atomic environment and show a complicated distribution as a function of i and of the position of the Fe atom. We note also that, when compared with the results presented in Figure 1, a more complex oscillatory behavior across the clusters is found for $L_\delta(i)$ together with a larger anisotropy, $\Delta L_{zx}(i) = L_z(i) - L_x(i)$, between the values obtained for the two considered orientations of the magnetization, which implies that the orbital magnetic moments at the Ni sites are very sensitive also to the chemical environment. Actually, we have found that, in contrast to the spin moments, the orbital moments of the Ni atoms surrounding the Fe impurities are most often considerably reduced when compared with the corresponding values in the pure Ni_{19} structure [compare for example $L_\delta(i)$ with $i = 5, 8, 9, 13$ in Figs. 1 and 2a]. However, sizable enhancements can be also observed at the more distant Ni sites [see for instance the results for $i = 1$ in Figs. 1 and 2a] a behavior that, on the average, only slightly affects the orbital moment per Ni atom in both $FeNi_{18}$ clusters ($\langle L_\delta \rangle \sim 0.18\ \mu_{\rm B}$/Ni).

As in the pure Ni_{19} cluster, we can appreciate both in Figures 2a and 2b the existence of values as large as 0.30 $\mu_{\rm B}$ for $L_\delta(i)$ at some Ni atoms, i.e., about 600% larger

than in the bulk. The orbital moment at the Fe site is most often enhanced (up to 180%) with respect to the measured bulk value [37], $L^{exp}_{\rm bulk}({\rm Fe}) = 0.092\ \mu_{\rm B}$, however it is considerably reduced when the Fe atom moves from the outermost shell to the interior of the structure, going from $0.17 \rightarrow 0.11 \rightarrow 0.08\ \mu_{\rm B}$ when the Fe atom is located in the second shell [Fig. 2a], in the first shell [Fig. 2b] and at the central site of the cluster (not shown), respectively. At this point, it is important to remark that in all the previous configurations for the $FeNi_{18}$ cluster, which roughly correspond to the limit of an Fe impurity in a nickel-rich environment, the orbital-to-spin ratios $\langle L_z\rangle/2\langle S_z\rangle$ for Fe are equal to 0.058, 0.037, and 0.03, respectively, which are very similar to the ratio $\langle L_z\rangle/2\langle S_z\rangle = 0.05 \pm 0.02$ for Fe measured by Foy et al. [32] in dilute random alloys of Fe in nickel by means of X-ray magnetic circular dichroism (XMCD). Finally we must say that, in contrast to the general behavior observed at Ni atoms, small anisotropies between the values of L_x and L_z at the Fe sites are always observed [see the results for $i = 18$ and 10 in Figs. 2a and 2b, respectively], a fact that anticipates small magnetic anisotropy energy contributions since according to reference [24] $L_z - L_x \propto E_x - E_z$, where $E_x - E_z$ is the variation of the total electronic energy when the orientation of the magnetization is rotated from the z- to the x-axis. Thus the local contributions of the Fe atoms are unimportant in determining the orientation of the global magnetization in the system.

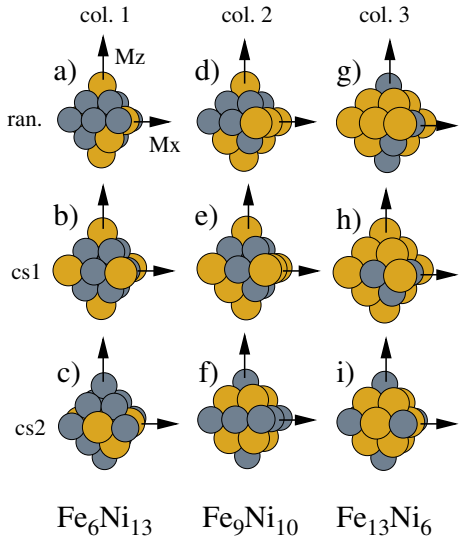

Fig. 3. Illustration of the cluster structures and chemical configurations for Fe_xNi_{19-x} ($x = 6, 9, 13$) cluster alloys. The structures shown in (a), (d), and (g) correspond to random (ran.) arrays of six, nine, and thirteen Fe atoms (light grey circles) included as substitutional impurities in the 19-atom cluster. (b), (e), and (h) define core-shell arrays (**cs1**) of six, nine, and thirteen Ni atoms (dark grey circles) clustered in the center of the structure surrounded by Fe atoms, and (c), (f), and (i) illustrate core-shell configurations (**cs2**) of six, nine, and thirteen Fe atoms covered by Ni species. The considered orientations of the magnetization are also shown.

3.2 Magnetism of fcc Fe_NNi_{19-N} cluster alloys (N = 6, 9, 13)

The results discussed in the previous section have already revealed the existence of an interesting behavior for the spin, orbital, and total magnetic moments in both Ni_{19} and $FeNi_{18}$ clusters as a function of the local geometrical and chemical environments. However, it is clear that when increasing the Fe content in the clusters, additional interesting phenomena may appear due to the increasing Fe−Ni interactions and appearance of Fe-rich regions in the clusters. Furthermore, it should be possible to analyze the role of the chemical ordering in the total magnetization of the particle and to quantify how the possible existence of random alloys or the clustering of a particular species in the structure affects the energy level spectra as well as the local moment distribution across the clusters. This fact might induce dramatic changes in the magnetic properties of the system.

The cluster structures, orientations of the magnetization, and the chemical configurations used in the calculations are illustrated in Figure 3. In the figure we consider again 19-atom Fe−Ni cluster alloys but having now 6, 9, and 13 iron atoms (denoted by light grey circles) incorporated as substitutional impurities which corresponds to 30, 47, and 68% of Fe content, respectively. The configurations (in which only the front view is presented) shown in Figures 3a, 3d, and 3g illustrate random arrays of Fe atoms, Figures 3b, 3e, and 3h correspond to core-shell arrays (**cs1**) in which Ni atoms are at the center surrounded by Fe atoms, while Figures 3c, 3f, and 3i show again core-shell configurations (**cs2**) in which now Fe atoms are clustered at the center covered by Ni atoms.

Let us emphasize that, similarly to the single impurity case, in the random and **cs1** configurations, the value of the average spin moment $2\langle S_z\rangle$ in both Fe_6Ni_{13} [Figs. 3a and 3b] and Fe_9Ni_{10} [Figs. 3d and 3e] clusters is independent of the chemical ordering, being the result of saturated-like contributions from both Ni ($\sim$1.0 $\mu_{\rm B}$) and Fe ($\sim$3.0 $\mu_{\rm B}$) atoms. The magnitude of $2\langle S_z\rangle$ increases with the Fe content giving values of 1.61 $\mu_{\rm B}$/atom for both configurations shown in Figures 3a and 3b and of 1.93 $\mu_{\rm B}$/atom for the alloys shown in Figures 3d and 3e. As already discussed in the previous section, the robustness of the energy level distribution around $\epsilon_{\rm F}$ is at the origin of this behavior. On the other hand, for the $Fe_{13}Ni_6$ random cluster alloy [see Fig. 3g], the high percentage of Fe content leads to the existence of some iron-clustering in well defined regions of the structures. This Fe aggregation in the particle induces the formation of nonsaturated local moments at the iron sites (a well-known tendency of pure iron clusters) that reduces also the spin magnetization at the Ni atoms. Even if for this larger content in Fe $2\langle S_z\rangle$ still increases, its magnitude is now more sensitive to the chemical ordering of the Fe and Ni atoms in the cluster alloys yielding values of 2.26 and 2.40 $\mu_{\rm B}$/atom for the configurations shown in Figures 3g and 3h, respectively.

As in the single Fe-impurity case, the different behavior for the average magnetization obtained between

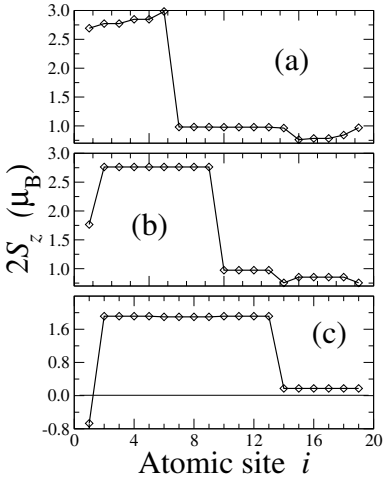

Fig. 4. Calculated local spin moments $2S_z(i)$ for (a) Fe_6Ni_{13}, (b) Fe_9Ni_{10}, and (c) $Fe_{13}Ni_6$ clusters. We show results only for **cs2** configurations as specified in col. 3 of Figure 3.

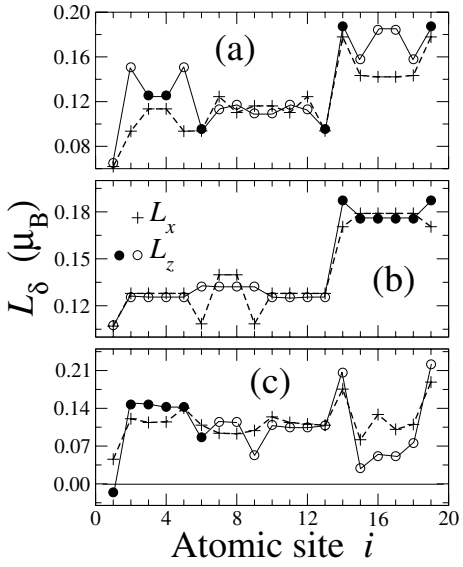

Fig. 5. Local orbital magnetic moments $L_\delta(i)$ as a function of the atom number i for Fe_6Ni_{13} clusters. We show results for (a) random, (b) **cs1**, and (c) **cs2** configurations as illustrated in col. 1 of Figure 3. The values of $L_\delta(i)$ at the Fe sites are specified by the filled circles.

Figures 3g and 3h can be explained by looking at the precise details of the DOS around the Fermi level in both alloys. In this case, by comparing the paramagnetic average DOS of the $Fe_{13}Ni_6$ cluster (not shown) in the random and core-shell **cs1** configurations, we have noted the existence of sizable differences between the two atomic distributions all along the electronic spectra, however, the most remarkable feature is that the value at the Fermi level for the **cs1** configuration is almost 30% larger than that found in the random array. Therefore, according to the Stoner theory we can expect that the magnetic moment of the core-shell **cs1** structure will be higher than in the random distribution. This is actually the behavior obtained when the calculation is performed by switching on both the considered exchange interactions as well as the SO contributions in our electronic Hamiltonian.

A more interesting situation occurs for the core-shell arrays in which the Fe atoms are clustered inside the particles (**cs2**). The local spin magnetization profiles for these chemical configurations are shown in Figure 4 where 6 [Fig. 4a], 9 [Fig. 4b], and 13 [Fig. 4c] Fe atoms are assumed to be located at the center of the structure. In these cases, even for the lowest Fe content shown in Figure 4a, appreciable local variations of $2S_z(i)$ are already observed both in iron- and nickel-rich regions, which is in contrast with the saturated values obtained for the configurations shown in Figures 3a and 3b. Indeed, the values of $2S_z(i)$ at the Fe sites vary now between 2.7–3.0 μ_B while at the Ni atoms we find values ranging from 0.75–0.98 μ_B. This behavior is similar to the local moment distribution obtained for the Fe-rich Fe−Ni random cluster alloys discussed in the previous paragraph where a small aggregation of Fe atoms in the structure [see Fig. 3g] was at the origin of the development of non saturated local moments in the particle. When increasing the Fe content we note from Figure 4b a sizable quenching of the spin magnetization at the Fe atom located at the center of the structure and finally, an antiparallel configuration sets in for 13 Fe-atoms [Fig. 4c], a behavior which can be compared with the well-known tendency to antiferromagnetic-like alignments of the local moments in γ fcc Fe [39], and that has been also observed in free uncovered small fcc Fe clusters by Lee et al. [40] as well as by Dorantes-Dávila and co-workers [41].

It is thus clear that, by increasing the concentration of Fe atoms in the **cs2** configuration, the average value of the spin magnetization in the clusters has a non monotonic behavior going from 1.52 → 1.72 → 1.21 μ_B when the Fe content varies from 30 [Fig. 4a] to 47 [Fig. 4b] to 68% [Fig. 4c]. In these configurations, the considerably reduced value for the average magnetization in the $Fe_{13}Ni_6$ structure [see Fig. 3i] is related to the appearance of a well defined fcc Fe-rich region having spin configurations with antiparallel arrays. Actually, it is important to comment that the magnetization of the iron core strongly influences the magnetic behavior of the surface Ni atoms, where the spin moments can be lowered to values as small as 0.2 μ_B in the $Fe_{13}Ni_6$ cluster alloy [Fig. 4c]. However, as will be discussed in the following sections, for the larger sizes we have found that, when increasing the number of Ni atoms covering the iron-rich cores, this significant quenching of the local moments will be restricted only to the nickel atoms near the Fe−Ni interface, the outermost Ni sites exhibiting a bulk-like value (∼0.6 μ_B) for $2S_\delta(i)$.

In Figures 5 and 6 we show now the behavior of the local orbital moments $L_\delta(i)$ for 19-atom Fe−Ni clusters having low and high Fe contents, respectively, with random, **cs1**, and **cs2** configurations. From both figures we note a complex behavior as a function of the concentration and chemical ordering within the clusters that precludes us from deriving simple general rules. As in previous cases, we found sizable enhancements of the orbital moments with respect to both Fe and Ni bulk values, that are most often more pronounced at the outermost atomic

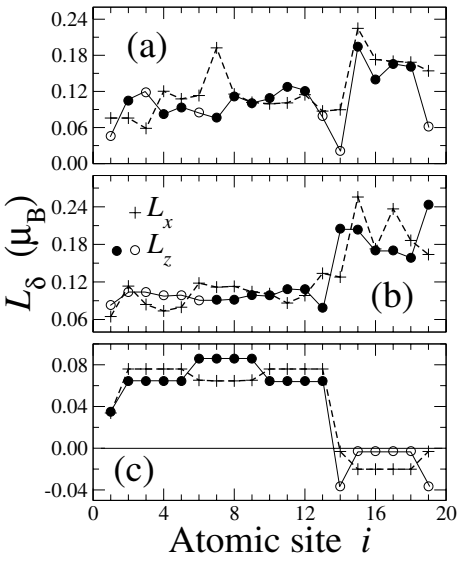

Fig. 6. Local orbital magnetic moments $L_\delta(i)$ as a function of the atom number i for $Fe_{13}Ni_6$ clusters. We show results for (a) random, (b) **cs1**, and (c) **cs2** configurations as illustrated in col. 3 of Figure 3. The values of $L_\delta(i)$ at the Fe sites are specified by the filled circles.

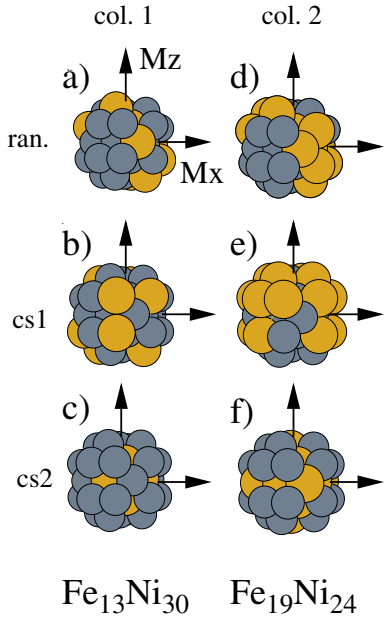

Fig. 7. Illustration of the cluster structures and chemical configurations for Fe_xNi_{43-x} ($x = 13, 19$) cluster alloys. The structures shown in (a) and (d) correspond to random (ran.) arrays of thirteen and nineteen Fe atoms (light grey circles) included as substitutional impurities in the 43-atom cluster. (b) and (e) define core-shell arrays (**cs1**) of thirteen and nineteen Ni atoms (dark grey circles) clustered in the center of the structure surrounded by Fe atoms, and (c) and (f) illustrate core-shell configurations (**cs2**) of thirteen and nineteen Fe atoms covered by Ni species. The considered orientations of the magnetization are also shown.

sites. Large anisotropies are sometimes found between the values of $L_\delta(i)$ for the two considered orientations of the magnetization, and finally, even if in pure solids the orbital moment is larger for Fe than for Ni, we note that this is no longer necessarily the case when they are alloyed to form small clusters.

Actually, it is interesting to look at the evolution of the orbital-to-spin ratio in our random cluster alloys [Figs. 5a and 6a] and to see how the sizable modifications in the local order as a function of the Fe content [namely: presence of relatively isolated Fe impurities for a low Fe content as shown Fig. 3a and the formation of iron-rich regions in the clusters as shown in Fig. 3g with 68% of Fe] is reflected in this experimentally accessible quantity. Besides, as already referred in the previous paragraphs, there are some XMCD measurements on disordered fcc Fe−Ni thin films as a function of the Fe content to which it would be interesting to compare our results. For the low, medium (not shown), and high concentration regimes of iron in our Fe−Ni clusters we obtain always the same $\langle L_z\rangle/2\langle S_z\rangle$ ratio for Fe, being thus independent of the alloy composition and approximately equal to 0.045. This value is similar to that measured by XMCD on disordered fcc Fe−Ni thin films at different degrees of Fe content [32] from which also a constant orbital-to-spin ratio for Fe was found to be equal to 0.05±0.02. On the other hand, for Ni we observe a more sensitive behavior in our cluster alloys in which the $\langle L_z\rangle/2\langle S_z\rangle$ value changes from 0.135 → 0.118 → 0.096 when we increase the Fe content from 30, to 47, and 68%, respectively. Interestingly we can notice that, for the low Fe content regime [Figs. 3a and 5a], our calculated $\langle L_z\rangle/2\langle S_z\rangle$ ratio for Ni is close to the value measured in disordered fcc Fe−Ni thin films which report a value of 0.14 ± 0.02 for Ni [32]. On the contrary, in the random $Fe_{13}Ni_6$ cluster, for which a highly interacting system with nonsaturated magnetic moments is obtained, our theoretical orbital-to-spin ratio for Ni is considerably reduced, being of the order of 0.09, a value that is comparable to the one measured in bulk-like nickel thin films (0.096) [42].

3.3 Magnetism of fcc Fe_NNi_{43-N} cluster alloys (N = 13 and 19)

We have considered also 43-atom nickel fcc clusters in which we have included 13 and 19 Fe atoms as substitutional impurities in random configurations [Figs. 7a and 7d] as well as in core-shell arrays where again Ni atoms are clustered in the center of the structures surrounded by Fe atoms [Figs. 7b and 7e] and vice-versa [Figs. 7c and 7f]. The decomposition of the spin moment S_z at each site of the structures and for the two considered orientations of the magnetization, as illustrated in Figure 7, reveals similar trends as the ones discussed in the previous sections. As a representative example, we would like to discuss the $Fe_{19}Ni_{24}$ cluster (44% of Fe content). In this case, we have found that the random alloy as well as the core-shell configuration in which the Ni atoms are located at the center of the $Fe_{19}Ni_{24}$ structure are characterized by the existence of saturated-like contributions from both Fe and Ni atoms. Thus their average spin magnetizations

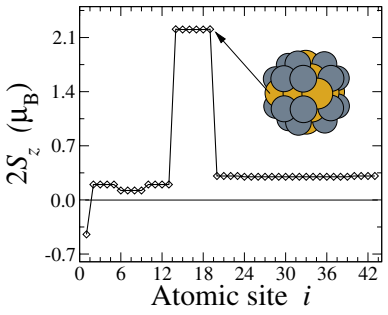

Fig. 8. Calculated local spin moments $2S_z(i)$ for the $Fe_{19}Ni_{24}$ cluster. We show results only for the **cs2** configuration as specified in col. 2 of Figure 7.

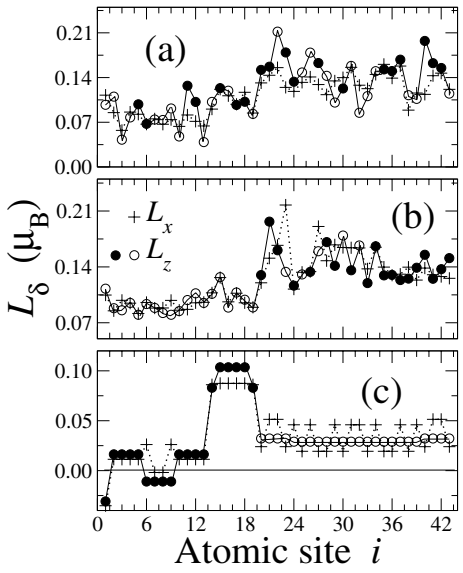

Fig. 9. Local orbital magnetic moments $L_\delta(i)$ as a function of the atom number i for $Fe_{19}Ni_{24}$ clusters. We show results for (a) random, (b) **cs1**, and (c) **cs2** configurations as illustrated in col. 2 of Figure 7. The values of $L_\delta(i)$ at the Fe sites are specified by the filled circles.

$2\langle S_\delta\rangle$ are approximately equal ($\sim$1.8 μ_B/atom). This value for $2\langle S_\delta\rangle$ is also almost the same as in the 19-atom cluster alloys shown in Figures 3a and 3b that have almost the same iron composition (47% of Fe content), in which an average spin magnetization of 1.72 μ_B/atom has been found. Finally, it is also close to the average magnetization measured in both Fe−Ni thin films and bulk alloy ($\sim$1.7 μ_B/atom) for that percentage of Fe content [32].

On the other hand, as we show in Figure 8, for the core-shell $Fe_{19}Ni_{24}$ cluster having an iron core [see Fig. 7f], we observe a more complex magnetization profile. As in previous cases, the central site is defined by $i = 1$, values from $i = 2-13$ specify atoms located at the first shell of neighbors, sites with $i = 14-19$ define the next nearest neighbors and finally, for $i = 20-43$, the outermost atomic shell is defined. In this case, we note again the formation of an antiparallel spin configuration in which the local moment at the central site is aligned in an opposite direction with respect to those obtained in the rest of the atoms of the structure. As already observed in Figure 4c, this behavior is related to the formation of a well defined iron-rich fcc region in the clusters. Notice that reduced values for the local spin moments at the Fe sites are found, especially on the nearest neighbors of the central atom, accompanied with a significant quenching in the spin moments at the surface Ni sites. Furthermore, we note well defined interface effects in Figure 8: the Fe atoms forming the last atomic shell of the embedded iron cluster ($i = 14-19$), which are characterized by a sizable reduction in their number of Fe−Fe pairs, have local spin moments with values as large as 2.2 μ_B, being remarkably increased when compared to the fcc Fe bulk value ($\sim$0.7 μ_B) and of the order of the one obtained for the bcc macroscopic iron structure ($\sim$2.1 μ_B). It is thus clear that the magnetization profile in Fe−Ni cluster alloys strongly depends on the chemical configurations of the Fe and Ni atoms within the structures, producing dramatic changes in the average spin magnetization of the clusters. Actually, the value of the average spin moment $2\langle S_z\rangle = 0.5$ μ_B/atom found in the **cs2** $Fe_{19}Ni_{24}$ cluster alloy [see Figs. 7 and 8] is considerably reduced when compared to the average values obtained from the random and **cs1** distributions ($2\langle S_z\rangle \sim 1.8$ μ_B/atom). However, as will be seen in the following, it is close to the experimentally obtained average magnetization in Fe−Ni ultrafine particles for that range of compositions.

The local orbital moments $L_\delta(i)$ in the 43-atom cluster with a 44% of Fe content and for the three considered chemical configurations are shown in Figure 9 from which it is obvious that the orbital moments, in contrast to the spin magnetization in random and **cs1** structures, strongly depend on the local geometrical and chemical environments. In fact, large fluctuations between the different sites are found and no tendency to a uniform orbital magnetization, as in the case of $S_z(i)$, is observed. From Figures 9a and 9b, $L_\delta(i)$ follows a clear trend with respect to the local coordination for both Fe and Ni. Indeed, the less coordinated sites located at the outermost atomic shell (sites with $i = 20-43$) are the ones with the largest enhancements relative to the bulk [values for $L_\delta(i)$ of the order of $\sim$0.2 μ_B at the Ni sites can be found]. However, when compared with the distributions shown in Figures 2, 5 and 6, we note an average decrease of $L_\delta(i)$ together with smaller anisotropies, $\Delta L_{zx}(i)$, between the two considered orientations of the magnetization, due to the increased electron delocalization and to the more spherical shape of the cluster. Note also that, similarly to $Fe_{13}Ni_6$, the average orbital moment is significantly smaller for the Fe-core cluster. It is also interesting to analyze the orbital-to-spin ratio in these bigger cluster alloys. On the one hand, for the random distributions with 30 and 44% of Fe content we obtain, as in previous cases, the same values of $\langle L_z\rangle/2\langle S_z\rangle$ for Fe, equal to 0.043. In the case of Ni, the existence of still a large number of isolated Fe atoms in the structures for the considered iron contents (no sizable Fe clustering is present) leads also to an almost constant value for $\langle L_z\rangle/2\langle S_z\rangle$ of the order of 0.13 and 0.12 in both $Fe_{13}Ni_{30}$ and $Fe_{19}Ni_{24}$ cluster

alloys. As previously discussed, these values are similar to those obtained from XMCD measurements in disordered Fe−Ni thin films [32] where a composition-independent orbital-to-spin ratio for Fe has been observed, together with a considerably enhanced value of $\langle L_z\rangle/2\langle S_z\rangle$ for Ni with respect to the bulk, and of the order of 0.14 ± 0.02.

4 Discussion

It is interesting to discuss also about the possible implications of the observed strong correlation between chemical order and magnetic behavior obtained in our model Fe−Ni cluster alloys on the magnetization measurements of Li et al. [10] performed on Fe−Ni ultrafine particles. However, it is important to underline first that, in the previous experiments, Fe−Ni particles with an average diameter of 30−35 nm have been produced, thus a size out of reach of computer calculations. Furthermore, there are some effects related to the chemical and magnetic structure of their surfaces that need to be mentioned. First, the particles were exposed to hydrogen, argon and air before the magnetic characterization and as a consequence, the possible presence of adsorbed gases on the surface is expected to yield already reduced values for the average magnetization. Second, complex non collinear spin configurations at the surface can be present due to a possible uneffective alignment of the moments by the applied magnetic field. Of course, both surface effects will tend to reduce the average magnetization and in fact, this is clearly reflected in the measurements for the pure Ni and Fe particles where the average magnetization has been found to be reduced by approximately 35 and 20%, respectively, with respect to the expected bulk values. However, as clearly stated by the authors of reference [10], when both Fe and Ni atoms are alloyed to form the ultrafine particles there should exist an additional factor leading to an extra quenching of the average magnetization that cannot be explained by the surface effects, since the saturation magnetization of the particles does not increase significantly with increasing Fe content as in the bulk Fe−Ni samples (see Fig. 8 of Ref. [10]). As stated by the authors of reference [10] the reason for this behavior is uncertain and we believe that the strong sensitivity of the magnetic properties of Fe−Ni clusters to the chemical order, already illustrated in the previous sections, could play an important role.

In Figure 10, we show our calculated values for $\langle M_z\rangle = 2\langle S_z\rangle + \langle L_z\rangle$ obtained for the different sizes, compositions, and chemical configurations considered in our work. By analyzing first our 19-atom cluster alloys (see the inset of the figure) we note that, for the random and **cs1** configurations we always obtain $\langle M_z\rangle$ values that linearly increase as a function of the Fe content and that are systematically larger than the Fe−Ni bulk measurements within the range of compositions studied, similarly to previous theoretical studies [12,13]. As already shown in the previous sections these high magnetization values are the result of saturated like contributions from both Fe and Ni sites. On the contrary, for the **cs2** configurations (see Fig. 3),

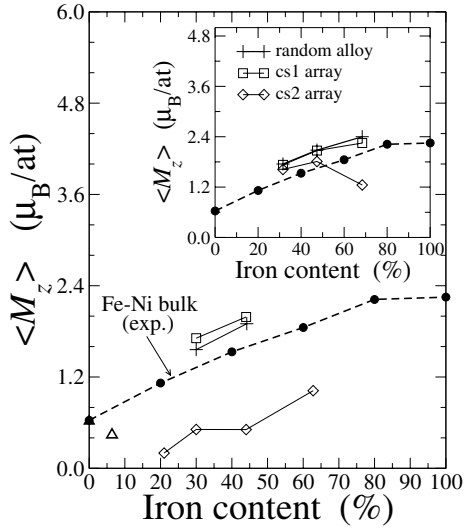

Fig. 10. Average total magnetic moment $\langle M_z\rangle$ [$\langle M_z\rangle = 2\langle S_z\rangle + \langle L_z\rangle$] of 43-atom Fe−Ni cluster alloys as a function of the Fe content and for different chemical configurations: random, **cs1**, and **cs2** (see Fig. 7). The filled and empty triangle-up symbols correspond to the results obtained for Ni_{201} and **cs2** $Fe_{13}Ni_{188}$ clusters (6.4% of Fe content). In the inset, we show similar results but for the 19-atom fcc structure. The experimental results from reference [10] for the average magnetization for bulk (filled circles) Fe−Ni alloys at different compositions are also shown. The lines are just guides to the eyes.

a non monotonic behavior as a function of the Fe content is observed and, as already seen from Figure 4, the existence of iron rich regions having nonsaturated local moments with antiparallel configurations are at the origin of this behavior. In particular, we note that our results for $\langle M_z\rangle$ in the $Fe_{13}Ni_6$ cluster (68.5% of Fe content) [Fig. 3i] clearly deviates from the Fe−Ni bulk data and becomes now considerably reduced.

Our calculations for the 43-atom cluster alloys (also shown in Fig. 10) clearly reveal that the strong correlation between chemical ordering and magnetism in Fe−Ni clusters results in a remarkable size- and environment-dependent magnetic behavior. We note the existence of high magnetization states for the random and **cs1** alloys as well as considerably reduced values for the **cs2** configurations which are characterized by well defined fcc iron-rich core regions. Actually, we can see that our values for $\langle M_z\rangle$ in the core-shell **cs2** arrays are quite comparable to the experimental findings in Fe−Ni nanoparticles for $Fe_{13}Ni_{30}$ (30.2% of Fe content) and $Fe_{19}Ni_{24}$ (44.2% of Fe content). These low values for $\langle M_z\rangle$ are also observed in the more dilute Fe_9Ni_{34} cluster and in the highly concentrated $Fe_{27}Ni_{16}$ structure having both **cs2** configurations and Fe contents of 21 and 62.3%, respectively, as well as in calculations for the more realistic **cs2** $Fe_{13}Ni_{188}$ structure (see the isolated empty triangle-up symbol for ∼6% of Fe content) where reduced magnetizations are also observed. In addition, we must emphasize that when compared with the value of $\langle M_z\rangle$ obtained for the pure Ni_{201} cluster (see

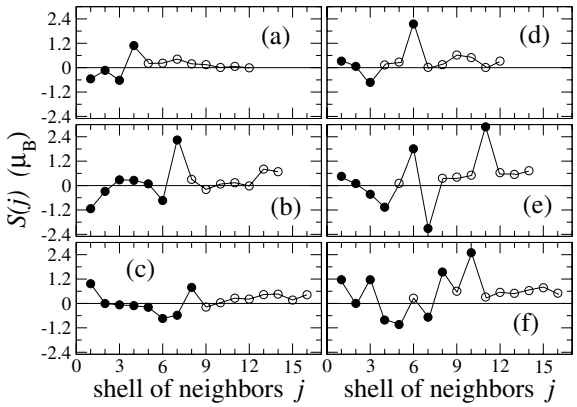

Fig. 11. Calculated local spin moments $S(j)$ at each shell of neighbors j for iron-rich core $Fe_{43}Ni_{158}$ [(a) and (d)], $Fe_{87}Ni_{156}$ [(b) and (e)], and $Fe_{135}Ni_{186}$ [(c) and (f)] nanoparticles. In the left column we show results for ideal core-shell configurations while, in the right column, core-shell nanoparticles having Fe−Ni interfaces with different degrees of intermixing are presented. The values of $S(j)$ at the atomic shells having only Fe species are specified by the filled circles.

the isolated filled triangle-up symbol), in which already a bulk value is found (0.62 μ_B/atom), the inclusion of only 6% of Fe in the center of the structure induces an appreciable reduction in the total magnetization of the particles.

Our results thus clearly reveal that the only type of chemical ordering leading to a significantly lowered magnetization in the clusters compared with the bulk alloys is a core shell structure with Fe atoms in the center of the fcc structure. Note that Fe and Ni atoms have similar surface energies and, as a consequence, upon alloying, it is not easy to establish a priori the existence of surface segregation in favor of a particular species. However, we would like to mention that Parks et al. [43] by analyzing the structure of gas phase Fe−Ni cluster alloys by means of the adsorption of molecular nitrogen on their surfaces concluded that the nickel-rich Fe−Ni alloy clusters tend to adopt the same geometrical structures as pure Ni clusters with the iron atoms located inside. In addition, the ab-initio calculations of Rao et al. [13] addressing the energetics and magnetic behavior of a single Ni impurity in an iron-rich environment concluded that it is more favorable for the nickel atom to reside at the cluster surface. It is thus clear that both previous experimental and theoretical results point towards the existence of a Ni surface segregation in real Fe−Ni cluster alloys.

Finally, it is advisable to analyze also the local moment distribution and the average magnetization of larger Fe−Ni structures having 201, 249, and 321 atoms. Following our results presented in the previous paragraphs we will consider only cluster arrays having iron-rich cores with 21, 35, and 42% of Fe content and, in order to avoid very large time-consuming computations, we will neglect the spin-orbit interaction in all cases. In Figures 11a, 11b, and 11c we show the behavior of the spin moment in each shell of neighbors for $Fe_{43}Ni_{158}$, $Fe_{87}Ni_{156}$, and $Fe_{135}Ni_{186}$ nanoparticles which actually confirms the trends discussed in the previous paragraphs. In all cases, we note the existence of complex magnetization profiles within the structures being defined by strong variations in the magnitude and changes of sign of the moments. As already observed in the small particle regime, we note that the iron cores are characterized by the presence of antiferromagnetic like ordering and for having local spin moments most often considerably reduced with respect to the bulk fcc value ($\sim$0.7 μ_B). Similarly also to the results of Figures 4 and 8, we notice how the reduced values of the magnetization in the Fe core is accompanied with a significant quenching of the local magnetization at the Ni sites. Actually, we have found that the lowering in the magnitude of the local moments at the surface atoms of the particles is highly dependent on the size and composition in the structures, being less effective when high magnetization states are obtained at the Fe sites closest to the Ni coating material [see Fig. 11b].

Concerning the behavior of the average magnetic moment per atom in the particles we have found an almost constant value in all three cases being of the order of 0.2 μ_B/atom. However, in this case we would like to comment that even if the Ni atoms would have been deposited on an already stabilized Fe core, it is very difficult in general to obtain high-quality core-shell nanoparticles [as the ones considered in Figs. 11a–11c] due to the possible existence of inhomogeneous growth or to the formation of internal interfaces having some degree of alloying [45]. In order to explore the role played by this last effect on the magnetic properties of our Fe−Ni cluster alloys, we have also performed some calculations for the same structures considered in Figures 11a–11c but for which we allow some intermixing between the last atomic shells of the Fe core and the first layers of the Ni coating. As we can see from the corresponding local moment distribution shown in Figures 11d–11f higher values for the spin moments are found in most of the sites compared to those of a perfect core-shell structure, resulting in an overall enhancement of the average magnetization in the nanoparticles. Actually, average values of 0.42, 0.45, and 0.62 μ_B/atom are obtained for the configurations shown in Figures 11d, 11e, and 11f, respectively.

5 Conclusion

In conclusion, we have systematically studied the magnetic behavior of several fcc Fe−Ni cluster alloys with different sizes (19−321 atoms), compositions and chemical configurations by using a d-band tight-binding Hamiltonian. We have found that significant variations in the composition and chemical order can have an important effect on the magnetic properties of the particles. Indeed high magnetization states are found in the random alloys as well as in core-shell arrays with a Ni core. On the contrary perfect core-shell arrays in which Fe atoms are clustered in the center of the structures have considerably reduced magnetizations. However, in this last case, the presence of some intermixing tends to increase the average magnetic moment. Our results might provide new insight into the

reduced values of the average magnetization observed in Fe−Ni nanoparticles [10] and suggesting a core-shell structure with an Fe core. Thus the knowledge of the chemical order in the Fe−Ni nanoparticles studied by Li et al. would be highly desirable to interpret their experimental results. More generally, the new features that appear in our bimetallic clusters give the hope that, by simply altering the composition ratios as well as the chemical ordering within the particles (e.g., by thermal treatments or low energy ion scattering experiments), it is possible to obtain various structures with different functionalities.

References

1. T. Taniyama, E. Ohta, T. Sato, M. Takeda, Phys. Rev. B **55**, 977 (1997)
2. C.K. Yee, R. Jordan, A. Ulman, H. White, A. King, M. Rafailovich, J. Sokolov, Langmuir **15**, 3486 (1999)
3. M.T. Reetz, W. Helbig, J. Am. Chem. Soc. **116**, 7401 (1994); R.M. Penner, J. Phys. Chem. B **106**, 3339 (2002)
4. S.E. Apsel, J.W. Emmert, J. Deng, L.A. Bloomfield, Phys. Rev. Lett. **76**, 1441 (1996)
5. I.M.L. Billas, A. Châtelain, W.A. de Heer, Science **265**, 1682 (1994)
6. A.J. Cox, J.G. Louderback, L.A. Bloomfield, Phys. Rev. Lett. **71**, 923 (1993); A.J. Cox, J.G. Louderback, S.E. Apsel, L.A. Bloomfield, Phys. Rev. B **49**, 12295 (1994)
7. D. Zitoun, M. Respaud, M.C. Fromen, M.J. Casanove, P. Lecante, C. Amiens, B. Chaudret, Phys. Rev. Lett. **89**, 037203 (2003)
8. G. Moraitis, H. Dreyssé, M.A. Khan, Phys. Rev. B **54**, 7140 (1996)
9. M. Respaud, J.M. Broto, H. Rakoto, A.R. Fert, L. Thomas, B. Barbara, M. Verelst, E. Snoeck, P. Lecante, A. Mosset, J. Osuna, T. Ould Ely, C. Amiens, B. Chaudret, Phys. Rev. B **57**, 2925 (1998)
10. X.G. Li, A. Chiba, S. Takahashi, J. Magn. Magn. Mater. **170**, 339 (1997)
11. G.J. Mankey, M.T. Kief, F. Huang, R.F. Willis, J. Vac. Sci. Technol. A **11**, 2034 (1993)
12. J. Guevara, A.M. Llois, Rev. Mex. Fis. **44**, 22 (1998)
13. B.K. Rao, S. Ramos de Debiaggi, P. Jena, Phys. Rev. B **64**, 024418 (2001)
14. M.B. Knickelbein, G.M. Koretsky, K.A. Jackson, M.R. Pederson, Z. Hajnal, J. Chem. Phys. **109**, 10692 (1998); M.B. Knickelbein, Annu. Rev. Phys. Chem. **50**, 79 (1999)
15. D.M. Cox, D.J. Trevor, R.L. Whetten, E.A. Rohlfing, A. Kaldor, Phys. Rev. B **32**, 7290 (1985)
16. R.A. Guirado-López, J. Dorantes-Dávila, G.M. Pastor, Phys. Rev. Lett. **90**, 226402 (2003)
17. K.W. Edmonds, C. Binns, S.H. Baker, S.C. Thornton, C. Norris, J.B. Goedkoop, M. Finazzi, N.B. Brookes, Phys. Rev. B **60**, 472 (1999); J.T. Lau, A. Föhlisch, R. Nietubyč, M. Reif, W. Wurth, Phys. Rev. Lett. **89**, 057201 (2002)
18. U. Wiedwald, M. Spasova, E.L. Salabas, M. Ulmeanu, M. Farle, Z. Frait, A. Fraile Rodríguez, D. Arvanitis, N.S. Sobal, M. Hilgendorff, M. Giersig, Phys. Rev. B **68**, 064424 (2003)
19. M.C. Desjonquères, D. Spanjaard, in *Concepts in Surface Physics*, edited by R. Gomer, Springer Series in Surface Science (Springer-Verlag, Berlin, 1993), Vol. 30
20. G.M. Pastor, J. Dorantes-Dávila, S. Pick, H. Dreyssé, Phys. Rev. Lett. **75**, 326 (1995)
21. J.L. Rodríguez-López, J. Dorantes-Dávila, G.M. Pastor, Phys. Rev. B **57**, 1040 (1998)
22. R. Félix-Medina, J. Dorantes-Dávila, G.M. Pastor, Phys. Rev. B **67**, 094430 (2003)
23. J. Friedel, P. Lenglart, G. Leman, J. Phys. Chem. Sol. **25**, 781 (1964)
24. P. Bruno, *Magnetismus von Festkörpern und Grenzflächen*, Ferienkurse des Forschungszentrums Jülich (KFA Jülich, 1993), ISBN 3–89336–110–3, Ch. 24
25. R. Haydock, in *Solid State Physics*, edited by H. Ehrenreich, F. Seitz, D. Turnbull (Academic, New York, 1980), Vol. 35, p. 215
26. V. Heine, Phys. Rev. **153**, 673 (1967)
27. V.L. Moruzzi, P.M. Marcus, in *Handbook of Magnetic Materials*, edited by K.H.J. Buschow (Elsevier, Science Publishers B.V., 1993), Vol. 7
28. P. Alvarado, J. Dorantes-Dávila, G.M. Pastor, Phys. Rev. B **58**, 12216 (1998)
29. M. Freyss, D. Stoeffler, H. Dreyssé, Phys. Rev. B **56**, 6047 (1997)
30. R.H. Victora, L.M. Falicov, T. Ishida, Phys. Rev. B **30**, 3896 (1984)
31. G.M. Pastor, J. Dorantes-Dávila, K.H. Bennemann, Phys. Rev. B **40**, 7642 (1989)
32. E. Foy, S. Andrieu, M. Finazzi, R. Poinsot, C.M. Teodorescu, F. Chevrier, G. Krill, Phys. Rev. B **68**, 094414 (2003)
33. T. Saha, I. Dasgupta, A. Mookerjee, Phys. Rev. B **50**, 13267 (1994)
34. J. Dorantes-Dávila, H. Dreyssé, G.M. Pastor, Phys. Rev. B **55**, 15033 (1997)
35. R. Guirado-López, Phys. Rev. B **63**, 174420 (2001)
36. H. Krakauer, A.J. Freeman, E. Wimmer, Phys. Rev. B **28**, 610 (1983); O. Hjortstam, J. Trygg, J.M. Wills, B. Johansson, O. Eriksson, Phys. Rev. B **53**, 9204 (1996)
37. M.B. Stearns, in *3d, 4d, 5d Elements, Alloys, Compounds*, edited by H.P.J. Wijn, Landolt-Börnstein, New Series (Springer-Verlag, Berlin, 1986), Group 3, Vol. 19, Pt. a
38. J.P. Pierce, J. Shen, R. Wu, Phys. Rev. B **65**, 132408 (2002)
39. S.C. Abrahams, L. Guttman, J.S. Kasper, Phys. Rev. **127**, 2052 (1962); W. Keune, R. Halbauer, U. Gonser, J. Lauer, D.L. Williamson, J. Magn. Magn. Mater. **6**, 192 (1977)
40. K. Lee, J. Callaway, K. Kwong, R. Tang, A. Ziegler, Phys. Rev. **31**, 1796 (1985)
41. J. Dorantes-Dávila, H. Dreyssé, G.M. Pastor, Phys. Rev. B **46**, 10432 (1992)
42. M.G. Samanat, J. Stöhr, S.S.P. Parkin, G.A. Held, B.D. Hermsmeier, F. Herman, M. Van Schilfgaarde, L.-C. Duda, D.C. Mancini, N. Wassdahl, R. Nakajima, Phys. Rev. Lett. **72**, 1112 (1994)
43. E.K. Parks, K.P. Kerns, S.J. Riley, Chem. Phys. **262**, 151 (2000)
44. Y.Z. Wu, H.F. Ding, C. Jing, D. Wu, G.L. Liu, V. Gordon, G.S. Dong, X.F. Jin, S. Zhu, K. Sun, Phys. Rev. B **57**, 11935 (1998)
45. G. Schmid, A. Lehnert, J.O. Malm, J.O. Bovin, Angew. Chem., Int. Ed. Engl. **30**, 874 (1991)